KOI-3278: A Self-Lensing Binary Star System

Ethan Kruse[1]* and Eric Agol[1]

Over 40% of Sun-like stars are bound in binary or multistar systems. Stellar remnants in edge-on binary systems can gravitationally magnify their companions, as predicted 40 years ago. By using data from the Kepler spacecraft, we report the detection of such a "self-lensing" system, in which a 5-hour pulse of 0.1% amplitude occurs every orbital period. The white dwarf stellar remnant and its Sun-like companion orbit one another every 88.18 days, a long period for a white dwarf–eclipsing binary. By modeling the pulse as gravitational magnification (microlensing) along with Kepler's laws and stellar models, we constrain the mass of the white dwarf to be ~63% of the mass of our Sun. Further study of this system, and any others discovered like it, will help to constrain the physics of white dwarfs and binary star evolution.

Einstein's general theory of relativity predicts that gravity can bend light and, consequently, that massive objects can distort and magnify more distant sources (*1*). This lensing effect provided one of the first confirmations of general relativity during a solar eclipse (*2*). Gravitational lensing has since become a widely used tool in astronomy to study galactic dark matter, exoplanets, clusters, quasars, cosmology, and more (*3*, *4*). One application has yet to be realized: In 1973, André Maeder predicted that binary star systems in which one star is a degenerate, compact object—a white dwarf, neutron star, or black hole—could cause repeated magnification of its companion star (instead of the standard eclipses) if the orbit happened to be viewed edge-on (*5*). The magnification of these self-lensing binary systems is small, typically a part in one thousand or less if the companion is Sun-like, and so it was not until high-precision stellar photometry was made possible with the Corot and Kepler spacecrafts that this could be detected (*6*, *7*). Stellar evolution models predict that about a dozen self-lensing binaries could be found by the Kepler spacecraft (*8*), but none have been discovered to date. A self-lensing binary system allows the measurement of the mass of the compact object, which is not true for most galaxy-scale microlensing events in which there is a degeneracy between the velocity, distance, and mass of the lensing object (*9*). Microlensing does affect several known white dwarfs in binaries in which the depth of eclipse is made slightly shallower (*10*–*14*) but does not result in brightening because occultation dominates over magnification at the short orbital periods of those systems.

Here, we report that Kepler Object of Interest 3278 (KOI-3278) (*15*, *16*), a term intended for planetary candidates, is instead a self-lensing binary composed of a white dwarf star orbiting a Sun-like star. The candidate planetary transit signal is actually the repeated occultation of the white dwarf as it passes behind its stellar companion. A search for other planets in this system with the Quasiperiodic Automated Transit Search algorithm (*17*) turned up a series of symmetric pulses, brightenings rather than dimmings, with a near-identical period and duration as the transit candidate but occurring almost half an orbital period later. All these properties can be explained by magnification of the Sun-like star as the white dwarf passes in front; 16 microlensing pulses were found, in addition to 16 occultations. The pulses and occultations are periodic and uniform in magnitude and duration (Fig. 1), which is consistent with a nearly circular, Keplerian orbit. Because there is no other phenomenon (that we know of) that can cause such a brief, symmetric, periodic brightening, we constructed a model for KOI-3278 composed of an eclipsing white dwarf and G dwarf (Sun-like star) binary (*18*).

Even without a full model, an estimate of the mass of the white dwarf, M_2, can be made directly from the light curve. The ratio of the fluence of the microlensing pulse, $F_{\rm pulse}$, to the stellar fluence over an orbital period, $F_{\rm tot}$, is given (*19*) by $F_{\rm pulse}/F_{\rm tot} = 5.4 \times 10^{-6}\sqrt{(1-b^2)}(M_2/M_\odot)(R_\odot/R_1)$, where R_1 is the radius of the G dwarf and b is the impact parameter (*20*). Because the duration of the pulse is 5 hours, the period is 88.18 days, and the magnification is 10^{-3}, we calculated $F_{\rm pulse}/F_{\rm tot}[1-(b/0.7)^2]^{-1/2} \approx 3.3 \times 10^{-6}$ and $M_2 \approx 0.6\,M_\odot$, which is a typical mass for a white dwarf star (*21*).

To jointly constrain the parameters of both stars, we fitted a full model simultaneously to the Kepler time-series photometry and the multiband photometry collected from other surveys (*18*). We modeled the light curve by using a Keplerian orbit with the gravitational lensing approximated as an inverted transit light curve, which is appropriate when the Einstein radius is small (*19*). We compared the Padova stellar evolution models (*22*) to the multiband photometry to constrain the properties of the G dwarf while accounting for extinction (A_V). Last, we used cooling models to constrain the age of the white dwarf (*23*).

Our model provides an accurate description of the data (Fig. 2) with a reduced χ^2 value of unity. From this model, we calculated the stellar parameters and the binary system's orbital properties (Table 1), with uncertainties derived from a Markov-chain Monte Carlo analysis (*18*). The model produced a white dwarf mass of $M_2 = 0.63\,M_\odot \pm 0.05\,M_\odot$, with a G dwarf companion of $M_1 = 1.04^{+0.03}_{-0.06}\,M_\odot, R_1 = 0.96^{+0.03}_{-0.05}\,R_\odot$, and effective temperature $T_{\rm eff,1} = 5568 \pm 39$ K: a star very similar to our Sun. Because the white dwarf, with its small size, is much fainter than the G dwarf, we cannot yet measure its temperature directly. However, given the measured mass from gravitational lensing, we inferred its size to be $R_2 =$

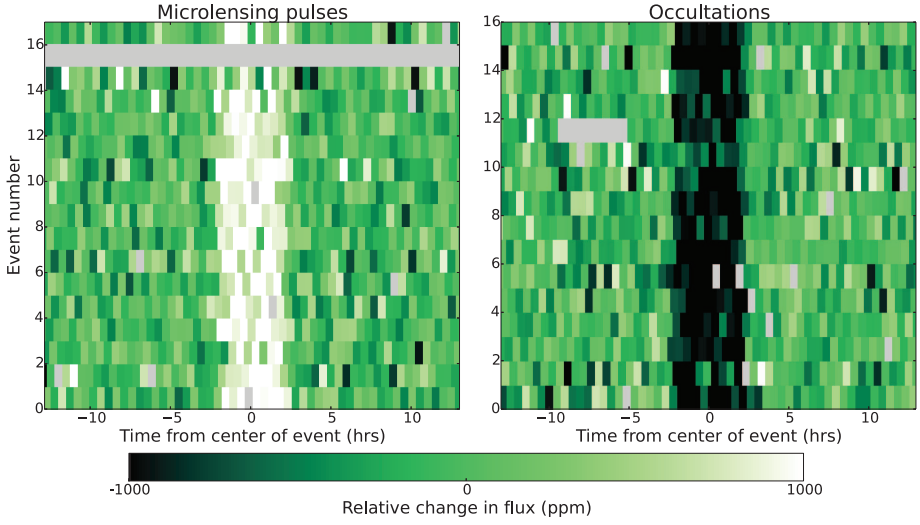

Fig. 1. Detrended flux versus time for all 16 microlensing pulses and 16 occultations in KOI-3278. Each row depicts the relative fluxes in 29.3-min Kepler cadences around an event. The rows are separated by the orbital period, $P = 88.18$ days. White represents brighter flux and black dimmer, whereas gray represents missing data or outliers that have been removed. ppm, parts per million.

[1]Department of Astronomy, University of Washington, Box 351580, Seattle, WA 98195, USA.

*Corresponding author. E-mail: eakruse@uw.edu

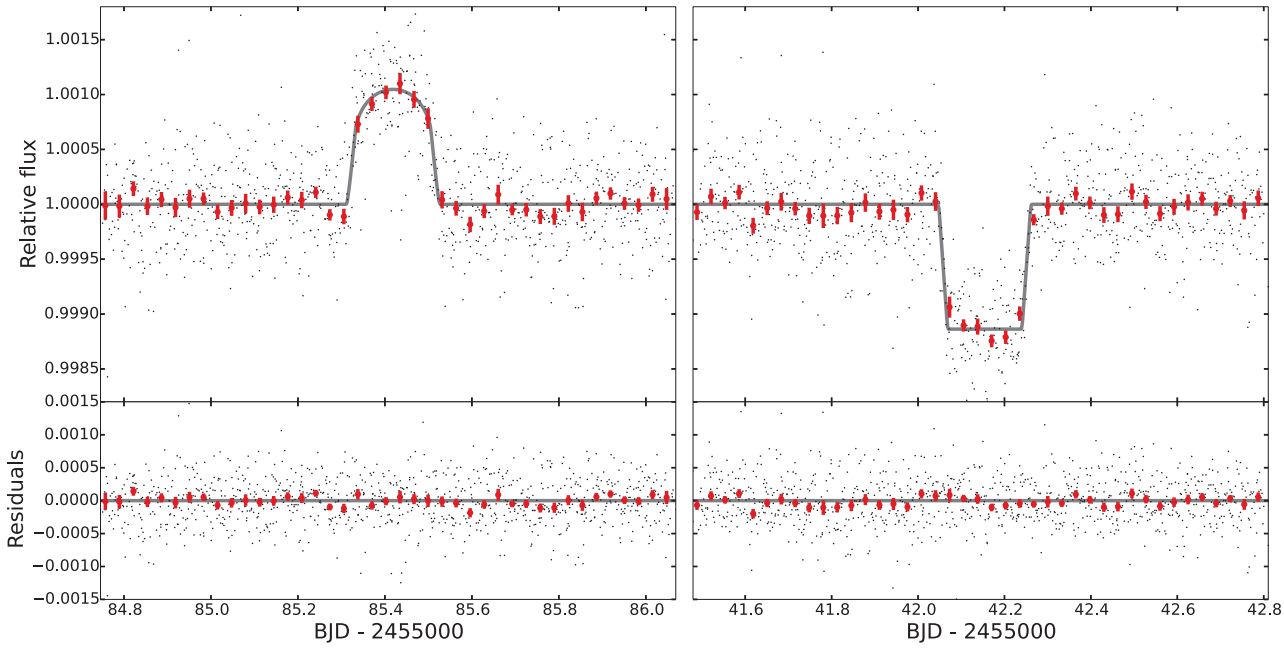

Fig. 2. Model fit to the data. Detrended and folded Kepler photometry of KOI-3278 presented as black points (all pulses and occultations have been aligned), overplotted with the best-fit model (gray line) for the microlensing pulse (**left**) and occultation (**right**). Red error bars show the mean of the folded data over a 45-min time scale. Bottom graphs show the residuals of the data with the best-fit model subtracted. BJD, barycentric Julian date.

0.0117 $R_\odot$ ± 0.0006 $R_\odot$ by using a mass-radius relation appropriate for carbon-oxygen white dwarfs. With a radius for the white dwarf, the measured occultation depth when it passes behind the G dwarf can be used to constrain the temperature of the white dwarf, which we found to be $T_{\mathrm{eff},2}$ = 10,000 ± 750 K; this temperature would give the white dwarf the bluish hue of an A star. The Einstein radius (R_E) is about twice the inferred size of the white dwarf, which allows lensing to dominate over occultation when the white dwarf passes in front. Gravitational lensing causes a distorted and magnified image of the G dwarf outside the Einstein ring in addition to a second inverted and reflected image of the G dwarf within the Einstein ring (Fig. 3); the inner image is partially occulted by the white dwarf's disk, reducing the observed magnification slightly.

Our model does not include the effect of star spots, but the Kepler G dwarf light curve displays their characteristic quasi-periodic fluctuations with a root mean square of 0.76%. We estimated that the spots would affect the derived stellar properties by less than a percent, smaller than the statistical errors in our model. Spot analysis revealed a G dwarf rotational period of P_{rot} = 12.5 ± 0.1 days. This short rotational period is expected for a G dwarf of only 0.89 ± 0.14 Gy (*18*). The white dwarf cooling time, t_{cool}, is 0.66 ± 0.06 Gy, which when added to the main sequence lifetime (t_2) of its progenitor with mass $M_{2,\mathrm{init}}$ gives a total age of the binary system of $t_1 = 1.6^{+0.9}_{-0.6}$ Gy; this age is marginally inconsistent (1.4σ) with the spin-down age of the G dwarf.

However, the G dwarf may have been spun up because of accretion of gas from the white dwarf progenitor. Because the white dwarf progenitor was previously a red giant, it should have enveloped the G dwarf during a common-envelope phase (*24*). The initial orbital period of the binary was likely several years long, and the period was likely shortened because of drag during the common-envelope phase. During this phase, the G dwarf accreted some gas from the red giant, increasing its mass by 10^{-3} to 10^{-2} $M_\odot$ and spinning the G dwarf up from the angular momentum contained in the accreted gas; this spin-up would have reset the age-spin relation, which could explain the slight age discrepancy.

KOI-3278 is the longest period eclipsing post-common-envelope binary found to date (fig. S7), and it is also one of the only examples of an eclipsing Sirius-like system—a binary composed of a noninteracting white dwarf and a Sun-like (or hotter) main-sequence star (*25*–*27*). As such, it will help to provide constraints on the physics of formation and evolution of short and intermediate period evolved binary stars, thereby improving our knowledge of the formation of accreting binaries and sources of gravitational waves. We expect that a few more self-lensing binaries will be found in the Kepler data at shorter orbital periods than KOI-3278. The magnification decreases down to periods of ≈16 days, making them more difficult to find; at even shorter periods, occultation by the white dwarf's disk wins out over the lensing, causing a shallower eclipse as in KOI-256 (*13*). Systems like KOI-3278 should not be a substantial source of false-positives for exoplanets;

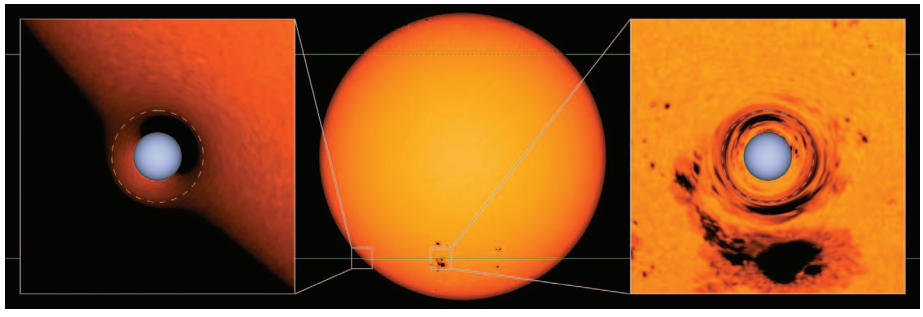

Fig. 3. Illustration of lensing magnification. (**Center**) The false-color disk of a G dwarf (using an actual image of the Sun from NASA/SDO HMI), in which the green line shows the trajectory of the white dwarf, with the dotted portion indicating where it passes behind the G dwarf. (**Left** and **right**) Close-ups of areas boxed in center show the lensed image of the G dwarf at two different times during the microlensing pulse; the white dwarf is the blue sphere. The white dashed line shows the Einstein ring of the white dwarf. The model that we fit to the data does not contain spots; however, the spots and granulation make the lensing distortion more apparent.

Table 1. Parameters of the KOI-3278 binary star system. More information can be found in the supplementary text. The median and 68.3% bounds are given for each parameter. g_1, surface gravity in cm/s^2. L_{WD}, luminosity of the white dwarf. e, eccentricity. ω, argument of periastron. a, semimajor axis. i, inclination. F_2/F_1 flux ratio between the white dwarf and G dwarf in the Kepler band. D, distance. σ_{sys}, systematic errors in the multiband photometry.

Variable	Value
G Dwarf	
M_1 ($M_\odot$)	$1.042^{+0.028}_{-0.058}$
R_1 ($R_\odot$)	$0.964^{+0.034}_{-0.054}$
$[Fe/H]_1$	$0.39^{+0.22}_{-0.22}$
t_1 (Gy)	$1.62^{+0.93}_{-0.55}$
$T_{eff,1}$ (K)	5568^{+40}_{-38}
$\log(g_1)$	$4.485^{+0.026}_{-0.020}$
White Dwarf	
$M_{2,init}$ ($M_\odot$)	$2.40^{+0.70}_{-0.533}$
M_2 ($M_\odot$)	$0.634^{+0.047}_{-0.055}$
$T_{eff,2}$ (K)	9960^{+700}_{-760}
R_2 ($R_\odot$)	$0.01166^{+0.00069}_{-0.00056}$
R_E ($R_\odot$)	$0.02305^{+0.00093}_{-0.00107}$
t_2 (Gy)	$0.96^{+0.90}_{-0.53}$
t_{cool} (Gy)	$0.663^{+0.065}_{-0.057}$
L_{WD} ($L_\odot$)	$0.00120^{+0.00024}_{-0.00023}$
Binary System	
P (days)	$88.18052^{+0.00025}_{-0.00027}$
t_0 (−2,455,000 BJD)	$85.4190^{+0.0023}_{-0.0023}$
$e\cos\omega$	$0.014713^{+0.000047}_{-0.000061}$
$e\sin\omega$	$0.000^{+0.049}_{-0.054}$
a (AU)	$0.4605^{+0.0064}_{-0.0103}$
a/R_1	$102.8^{+3.7}_{-2.4}$
b_0	$0.706^{+0.020}_{-0.025}$
i (deg)	$89.607^{+0.026}_{-0.020}$
F_2/F_1	$0.001127^{+0.000039}_{-0.000039}$
D (pc)	808^{+36}_{-49}
σ_{sys} (mags)	$0.0246^{+0.0127}_{-0.0078}$
K_1 (km/s)	$21.53^{+0.96}_{-0.98}$
π (milli–arc sec)	$1.237^{+0.079}_{-0.053}$
α_1 (milli–arc sec)	$0.2169^{+0.0076}_{-0.0072}$
A_V (mags)	$0.206^{+0.017}_{-0.016}$

only one was predicted to be found in the Kepler data with its magnification of ≈0.1% (*8*).

Follow-up observations should better constrain the parameters of the white dwarf star in KOI-3278, allowing a test of the mass-radius relation for white dwarfs (*28*, *29*). Once the Kepler field rises (it had set before we detected the microlensing signal), radial velocity observations should show a semi-amplitude K_1 of 21.5 km/s and a line-broadening of 4 km/s. High-resolution spectroscopy will also better constrain the atmospheric properties of the G dwarf; in particular, spectral abundance anomalies caused by accretion of nuclear-processed material from the white dwarf progenitor should be sought. Measurements of the occultation of the white dwarf in the ultraviolet (with the Hubble Space Telescope) should appear much deeper, as much as 60% in depth as opposed to the 0.1% occultation depth in the Kepler band, and will yield constraints on the radius and temperature of the white dwarf. High angular resolution imaging would allow for better constraints to be placed on the presence of a third star in the system (*18*). Last, parallax measurements (π) with the Gaia spacecraft (*30*) will improve the precision of the properties of the G dwarf; Gaia can also detect the reflex motion of the G dwarf α_1 as it orbits the center of mass with the white dwarf. This provides another means to detect systems like KOI-3278 with inclinations that do not show microlensing or occultation; there are likely 100 of these among the Kepler target stars alone, given the ~1% geometric lensing probability of KOI-3278.

References and Notes

1. A. Einstein, *Science* **84**, 506–507 (1936).
2. F. W. Dyson, A. S. Eddington, C. Davidson, *Philos. Trans. R. Soc. London Ser. A* **220**, 291–333 (1920).
3. J. Wambsganss, *Living Reviews in Relativity* **1**, 12 (1998).
4. P. Schneider, C. Kochanek, J. Wambsganss, *Gravitational Lensing: Strong, Weak and Micro* (Saas-Fee Advanced Course 33, Springer, Berlin, 2006).
5. A. Maeder, *Astron. Astrophys.* **26**, 215 (1973).
6. E. Agol, *Astrophys. J.* **579**, 430–436 (2002).
7. K. C. Sahu, R. L. Gilliland, *Astrophys. J.* **584**, 1042–1052 (2003).
8. A. J. Farmer, E. Agol, *Astrophys. J.* **592**, 1151–1155 (2003).
9. B. Paczyński, *Annu. Rev. Astron. Astrophys.* **34**, 419–459 (1996).
10. T. R. Marsh, *Mon. Not. R. Astron. Soc.* **324**, 547–552 (2001).
11. J. D. R. Steinfadt, D. L. Kaplan, A. Shporer, L. Bildsten, S. B. Howell, *Astrophys. J.* **716**, L146–L151 (2010).
12. J. F. Rowe *et al.*, *Astrophys. J.* **713**, L150–L154 (2010).
13. P. S. Muirhead *et al.*, *Astrophys. J.* **767**, 111 (2013).
14. D. L. Kaplan *et al.*, *Astrophys. J.* **780**, 167 (2014).
15. C. J. Burke *et al.*, *Astrophys. J. Suppl. Ser.* **210**, 19 (2014).
16. P. Tenenbaum *et al.*, *Astrophys. J. Suppl. Ser.* **211**, 6 (2014).
17. J. A. Carter, E. Agol, *Astrophys. J.* **765**, 132 (2013).
18. Materials and methods are available as supplementary materials on *Science* Online.
19. E. Agol, *Astrophys. J.* **594**, 449–455 (2003).
20. The impact parameter is the projected sky separation of the white dwarf and G dwarf at midpulse, in units of the radius of the G dwarf; we find a best-fit value of $b = 0.7$ based on the full model fit. This formula assumes a circular orbit, neglects limb-darkening, and neglects obscuration by the white dwarf; whereas these effects (although minor) are accounted for in our full model.
21. S. O. Kepler *et al.*, *Mon. Not. R. Astron. Soc.* **375**, 1315–1324 (2007).
22. A. Bressan *et al.*, *Mon. Not. R. Astron. Soc.* **427**, 127–145 (2012).
23. P. Bergeron *et al.*, *Astrophys. J.* **737**, 28 (2011).
24. N. Ivanova *et al.*, *Astron. Astrophys. Rev.* **21**, 59 (2013).
25. A. Rebassa-Mansergas *et al.*, *Mon. Not. R. Astron. Soc.* **423**, 320–327 (2012).
26. M. Zorotovic, M. R. Schreiber, *Astron. Astrophys.* **549**, A95 (2013).
27. J. B. Holberg, T. D. Oswalt, E. M. Sion, M. A. Barstow, M. R. Burleigh, *Mon. Not. R. Astron. Soc.* **435**, 2077–2091 (2013).
28. J. L. Provencal, H. L. Shipman, E. Hog, P. Thejll, *Astrophys. J.* **494**, 759–767 (1998).
29. S. G. Parsons *et al.*, *Mon. Not. R. Astron. Soc.* **420**, 3281–3297 (2012).
30. M. A. C. Perryman *et al.*, *Astron. Astrophys.* **369**, 339–363 (2001).

Acknowledgments: E.K. was funded by an NSF Graduate Student Research Fellowship. E.A. acknowledges funding by NSF Career grant AST 0645416; NASA Astrobiology Institute's Virtual Planetary Laboratory, supported by NASA under cooperative agreement NNH05ZDA001C; and NASA Origins of Solar Systems grant 12-OSS12-0011. Solar image courtesy of NASA/Solar Dynamics Observatory (SDO) and the Helioseismic and Magnetic Imager (HMI) science teams. The Kepler data presented in this paper were obtained from the Mikulski Archive for Space Telescopes (MAST). The code used for analysis is provided in a repository at https://github.com/ethankruse/koi3278. The authors welcome requests for additional information regarding the material presented in this paper.

Supplementary Materials

www.sciencemag.org/content/344/6181/275/suppl/DC1
Materials and Methods
Supplementary Text
Figs. S1 to S7
Table S1
References (*31*–*84*)

10 February 2014; accepted 25 March 2014
10.1126/science.1251999

An Earth-Sized Planet in the Habitable Zone of a Cool Star

Elisa V. Quintana,[1,2]* Thomas Barclay,[2,3] Sean N. Raymond,[4,5] Jason F. Rowe,[1,2] Emeline Bolmont,[4,5] Douglas A. Caldwell,[1,2] Steve B. Howell,[2] Stephen R. Kane,[6] Daniel Huber,[1,2] Justin R. Crepp,[7] Jack J. Lissauer,[2,8] David R. Ciardi,[9] Jeffrey L. Coughlin,[1,2] Mark E. Everett,[10] Christopher E. Henze,[2] Elliott Horch,[11] Howard Isaacson,[12] Eric B. Ford,[13,14] Fred C. Adams,[15,16] Martin Still,[3] Roger C. Hunter,[2] Billy Quarles,[2] Franck Selsis[4,5]

The quest for Earth-like planets is a major focus of current exoplanet research. Although planets that are Earth-sized and smaller have been detected, these planets reside in orbits that are too close to their host star to allow liquid water on their surfaces. We present the detection of Kepler-186f, a 1.11 ± 0.14 Earth-radius planet that is the outermost of five planets, all roughly Earth-sized, that transit a 0.47 ± 0.05 solar-radius star. The intensity and spectrum of the star's radiation place Kepler-186f in the stellar habitable zone, implying that if Kepler-186f has an Earth-like atmosphere and water at its surface, then some of this water is likely to be in liquid form.

In recent years, we have seen great progress in the search for planets that, like our own, are capable of harboring life. Dozens of known planets orbit within the habitable zone (HZ), the region around a star within which a planet can sustain liquid water on its surface (*1*–*4*). Most of these HZ planets are gas giants, but a few, such as Kepler-62f (*5*), are potentially rocky despite having a larger

KOI-3278: A Self-Lensing Binary Star System

Ethan Kruse and Eric Agol

Science **344** (6181), 275-277.
DOI: 10.1126/science.1251999

Starry Brightness

The high photometric precision of NASA's Kepler observatory has enabled the detection of many planets because they cause slight dimming of their host stars as they orbit in front of them. From these data, **Quintana *et al.*** (p. 277) have spotted a five-planet system around a small star. Here, the outermost planet is only 10% larger than Earth and completes its 130-day orbit entirely within the habitable zone, where liquid water could exist on its surface. Similarly, Kepler can detect faint periodic brightenings, as **Kruse and Agol** (p. 275) have reported for the binary system KOI-3278. In this system, a white dwarf acts as a gravitational microlens when it passes in front of its Sun-like G-star companion every 88 days. The lensing effect allows the mass of the white dwarf to be estimated, which helps us to understand how similar binary systems may have evolved.